Scale effects in the bearing capacity of granular soils

Les effets d'échelle sur la capacité portante dans les sols granuleux

M.D.BOLTON, Cambridge University, UK
C.K.LAU, Cambridge University, UK

SYNOPSIS The drained strength of a variety of soils is shown to be well-represented by a linear reduction of secant φ with the logarithm of mean effective stress. Methods are presented for the calculation of bearing capacities appropriate to any given size of footing. Model tests of circular footings on two homologous soils under both enhanced surcharge and centrifugally enhanced self-weight are used to validate the new approach.

1 SOIL PROPERTIES

A number of anomalies still prevent the secure prediction of the penetration resistance of simple footings such as circular spuds supporting off-shore jack-up rigs. Many authors have referred to the observed dependence of bearing capacity coefficients on the size of a footing, or on the stress magnitude it induces in the soil. Such dependence must, however, be related not to lengths or to stresses but to dimensionless groups.

Two crushed silica soils were created which were similar in particle shape and aggregate geometry, but which differed by a factor of 50 in particle size: see figure 1 and table 1. These highly angular soils, referred to hereafter as sand and silt, were intended to reveal the effects of the ratio of particle size to footing size. Drained triaxial compression tests were conducted on dense (I_D = 1) samples of each soil at a range of effective cell presures between 10 kPa and 10 MPa. Curves of secant φ_{mob} and dilation $-\varepsilon_v$ are plotted against axial strain in figure 2. Figure 3a then shows the variation of secant φ_{max} with the logarithm of the mean stress p' at that instant. The data for the sand agree well with a previously published correlation for quartz sands (Bolton, 1986) against relative density I_D and p' in kPa:

$$\varphi_{max} - \varphi_{crit} = A[I_D(Q - \ln p') - 1] \qquad (1)$$

with Q = 10.0 and the factor A 3° in axisymmetric strain and 5° in plane strain. The silt displayed consistently less crushable particle contacts, and maintained dilatancy upto a much higher stress, following a parallel relation with Q = 11.6 . The critical state is reached from a relative density I_D at a mean stress given by $\ln p'_{crit} = Q - 1/I_D$.

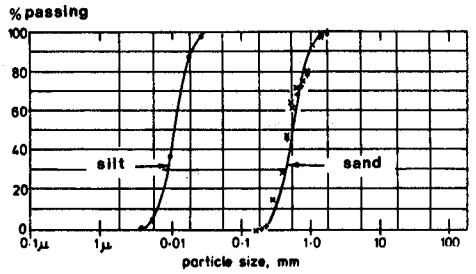

Figure 1 Grading curves of model soils

For comparison, a dense calcareous sand from the Halibut platform in the Australian Bass Strait (Airey et al, 1988) apparently followed a parallel relation with Q reduced to 8.8 by virtue of its smaller resistance to crushing. In each of these cases, the quality of fit using secant φ_{max} and log p' is much more satisfactory than would have been the case with a single straight Mohr-Coulomb envelope, as may be appreciated in figure 3b.

2 PLANE PLASTICITY CALCULATIONS WITH VARYING φ AND γ=0

When φ is taken to vary, two related values must be derived: φ_{op} is operative in the stress-rotation relation while φ_{en} defines the local tangent to the strength envelope as shown in figure 4, so that stress characteristics emerge at $\pm(\pi/4 - \varphi_{en}/2)$ to the major principal stress direction.

In plane strain, the mean effective stress in the plane of shearing s'=p'. Then from equation 1:

$$d\varphi/ds' = -A/s' \qquad (2)$$

where A is a constant. Lau (1988) shows:

$$\varphi_{en} = \sin^{-1}(\sin\varphi - A\cos\varphi) \qquad (3)$$

Taking ϑ to be the rotation of stress direction in a solution by the method of characterisics, it can also be shown that:

$$ds'/s' = \tan\varphi d\varphi \pm \sqrt{(\sec^2\varphi d\varphi^2 + 4\tan^2\varphi d\vartheta^2)} \qquad (4)$$

Substituting (2) into (4) we derive

$$\frac{ds'}{s'} = \pm \frac{2\tan\varphi \; d\vartheta}{\sqrt{(1+2A\tan\varphi - A^2)}} \qquad (5)$$

Table 1

	silt	sand
SiO_2	>99%	>97%
G_s	2.65	2.65
roundness R	0.40	0.41
sphericity S	0.80	0.77
d_{50} μm	12	600
k mm/s	3×10^{-4}	1.7
φ'_{crit} °	37.5	37.5

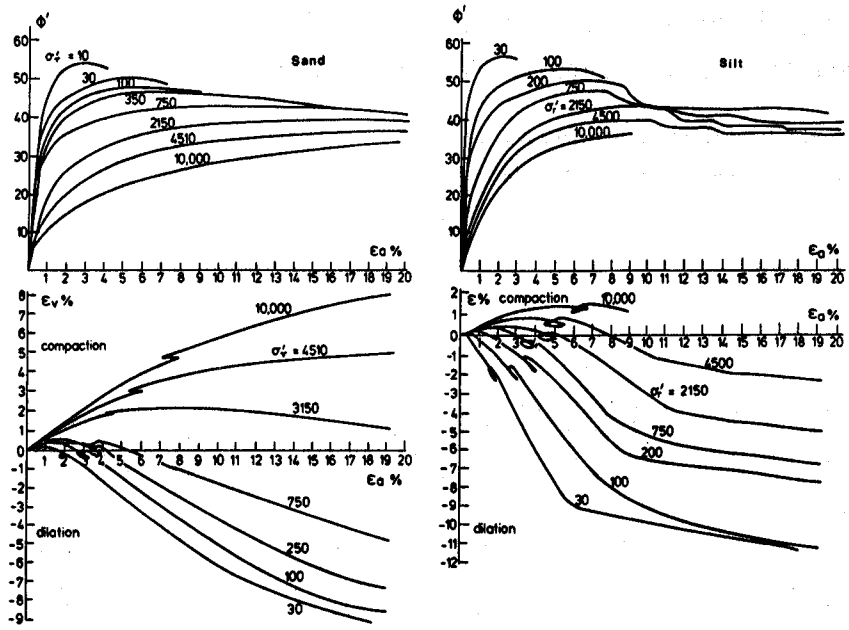

Figure 2 Drained triaxial compression tests

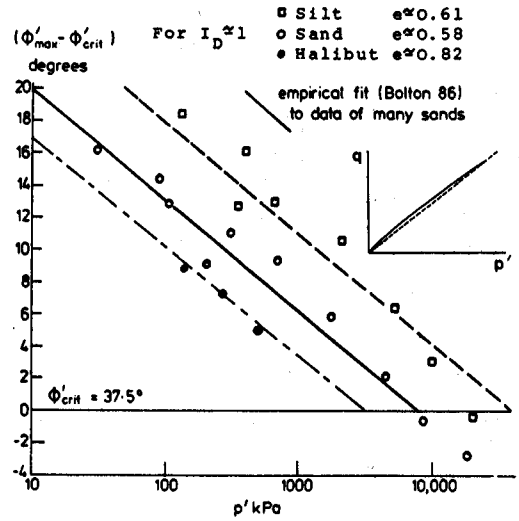

Figure 3 φ_{max} versus logarithm of mean stress

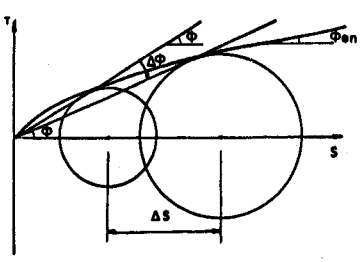

Figure 4 Secant φ

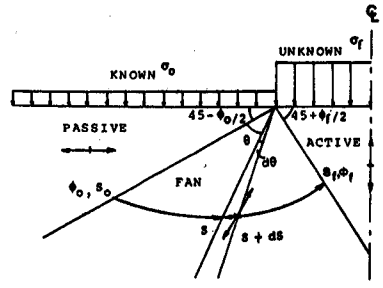

Figure 5 N_q bearing capacity problem

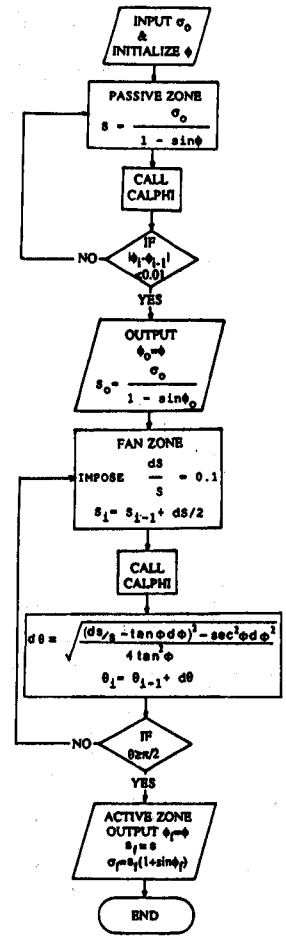

Figure 6 Flowchart for N_q calculation

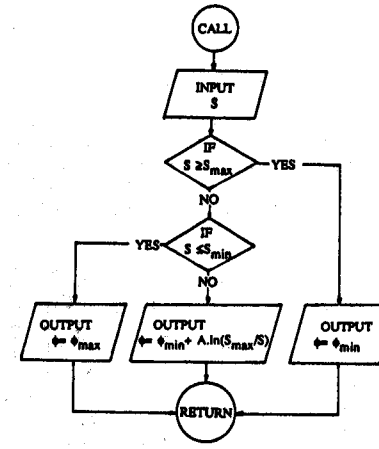

Figure 7 Routine to select φ

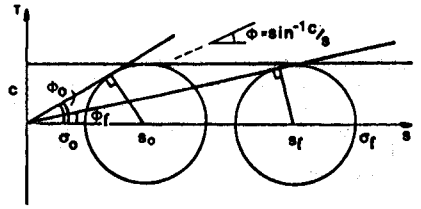

Figure 8 Variable φ relation to give equivalent c

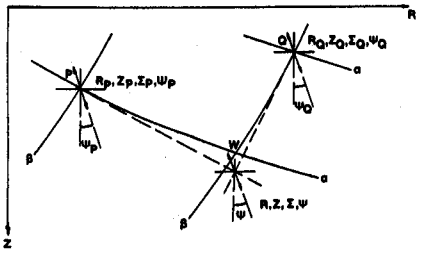

Figure 9 Axisymmetrical plastic analysis

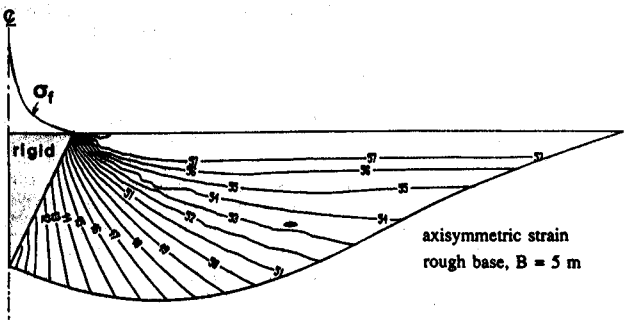

Figure 11 Distributions of φ and σ_f for Nγ problem

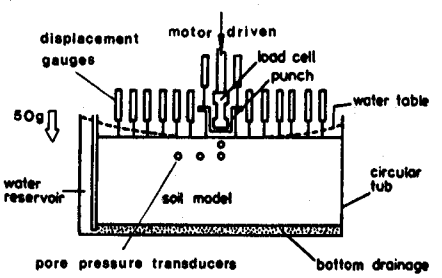

Figure 12 Model footing apparatus

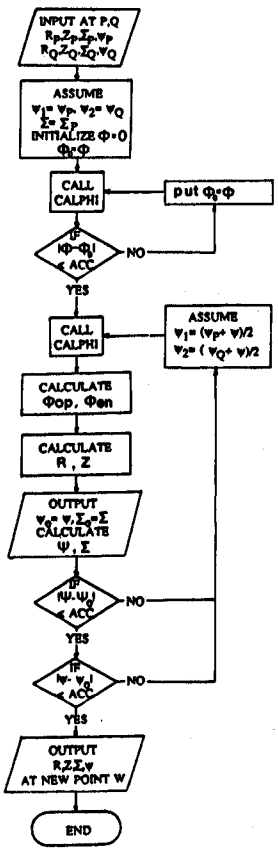

Figure 10 Flowchart for characteristic solution

Table 2		B/m			
		Sand		Silt	
		P_{crit}=8000 kpa		P_{crit}=40000 kpa	
φ	$N_{\gamma,rough}$	Calc.	Exp.	Calc.	Exp.
35	82.4				
36	100.8				
37	123.9				
38	153.1	10.00			
39	190.2	5.00			
40	237.6	3.00	5.00		
41	298.9			10.00	5.00
42	378.7	1.42			
43	480.5	0.90		5.00	3.00
44	619.4	0.40		3.00	
45	802.6			1.42	1.42
46	1051.8			0.90	
47	1384.2			0.40	
48	1847.3				
49	2491.5				
50	3403.4				
Col. 1	2	3	4	5	6

Table 3		σ_o/kpa				
		Sand			Silt	
		P_{crit} = 8000 kpa			P_{crit} = 40000 kpa	
φ	N_q	calc.	exp.		calc.	exp.
			B=100	B=14.2		B=14.2
35	61.0					
36	71.3					
37	82.8					
38	98.9					
39	116.4	200				
40	139.6			200		
41	165.8	100				200
42	200.4	50		100		
43	241.0		25		200	100
44	294.7	25		50	100	
45	359.3		10	25		50
46	443.5	10		10	50	25
47	550.0	5	5		25	10
48	686.3					
49	864.3				10	5
50	1103.3				5	
51	1427.1					
52	1853.7					
Col. 1	2	3	4	5	6	7

The square-root term modifies the usual constant-φ solutions, so we may define an operational value φ_{op}:

$$\tan\varphi_{op} = \tan\varphi/\sqrt{(1+2A\tan\varphi-A^2)} \qquad (6)$$

Substituting $A = 3 \times \pi/180$ we find that φ_{op} is between 1° and 2° smaller than φ for dense soil. Equation 5 can then be used in standard numerical integrations for soils which satisfy equation 1, with values of φ_{op} varying with stress just as φ varies.

An example calculation, for the bearing capacity factor N_q, is based on figure 5, and itemised in figure 6. The value of φ is continually updated according to the local estimate of s', using the routine of figure 7, which permits a linear increment of φ for a log decrement in s', within limits φ_{min} and φ_{max}.

The calculation method was checked by inserting a different secant-φ variation, $\sin\varphi = c/s$, which generates the simple cohesion envelope shown in figure 8. An identical approach deriving $\varphi_{en} = 0$ and $\varphi_{op} = \tan^{-1}(\sin\varphi)$ led to a numerical solution

$$\sigma_f - \sigma_o = 5.145\ c$$

which differs from the exact solution by only 0.07%.

3 AXISYMMETRIC PLASTICITY CALCULATIONS WITH VARYING φ

Figure 9 shows, in cylindrical coordinates, the normalised parameters used by Cox (1962) to solve bearing capacity problems for circular footings on heavy soil with constant φ, following the similar method for plane problems first set out by Sokolovski. New intersections of the stress characteristics are found by successive approximation, satisfying both geometry and Cox's stress-rotation equations: see figure 10.

Replacing φ by φ_{op} or φ_{en} (as appropriate) in Cox's equations, modified bearing capacity solutions emerge in which the secant φ_{max} varies around the footing in a realistic way. Figure 11 shows the outcome, for example, of an N_γ analysis for a rough, circular footing of 5m diameter, on the assumption of a rigid active cone beneath. φ_{max} varies from 36° in the highly stressed region to 57° near the soil surface, covering the whole range of data in figure 3.

Table 2 assembles the bearing capacity coefficients calculated for various footing diameters, and for the two model soils at $I_D = 1$. In order to select a value, it is first necessary to choose an appropriate value of p'_{crit} for the material. The correct value of N_γ in column 2 is then found against the appropriate footing diameter in column 3 or 5. The value of φ in column 1 is that constant value which would give the same value for N_γ in a conventional calculation.

Table 3 performs a similar function for N_q in relation to the magnitude of surcharge σ_o in columns 3 and 5. It should be noted that the relations between φ and both N_q and N_γ embodied in columns 1 and 2 of the tables are the result of applying Cox's constant-φ theory. The values of N_q and N_γ are larger than those derived for strip footings, and remain somewhat larger even when conventional shape factors are additionally applied. It may also readily be perceived that Meyerhof's simple rule that an equivalent constant φ be determined through a triaxial test at $p' = \sigma_f/10$ is not generally applicable over the whole range of bearing capacities listed in tables 2 and 3.

As before, this calculation procedure was checked for a secant-φ variation representing cohesion c. A bearing capacity factor $N_c = 5.63$ was derived, being within 1% of the value 5.69 quoted for perfectly plastic materials by Shield (1955).

4 EXPERIMENTAL VALIDATION

Figure 12 shows the experimental package used to investigate the validity of the foregoing method of calculation. Rough footings of diameter 14 or 100 mm could be forced very slowly into circular specimens of saturated soil, in order to record force against penetration. Dense specimens of sand (e=0.58, $I_D \approx 1$) were prepared dry by slow pluviation and then saturated from below. Dense specimens of silt (e=0.61, $I_D \approx 1$) were prepared by vibration in a saturated condition. Tests were conducted either under the surcharge of a rubber bag pressurised so that soil self-weight was negligible, or with centrifugally enhanced self-weight and an equivalent surcharge due solely to penetration.

Some of the resulting data were included in columns 4 and 6 of tables 2 and 3. The centrifuge tests are reported in table 2 at prototype scale, having scaled footing size by the acceleration factor. It will be seen in table 2 that the axisymmetric variable-φ theory predicts the measured N_γ within ±30%, but this represents an accuracy in φ of better than 1° (see column 1). There is a similar scatter in the prediction of N_q in table 3, by amounts corresponding to between 0 and 2° in φ. The average error in prediction for all the tests included in tables 2 and 3 amounts to 1° in φ, which is comparable to the scatter in figure 3.

It is clear that the small deviations between theory and experiment are of the same magnitude and tendency for both the sand and the silt. The fifty-fold difference in footing/particle size ratio has apparently introduced no extraneous effects: previously reported "scale effects" were presumably due solely to differences in the ratio of applied stress to the soil crushing stress.

5 CONCLUSIONS

1. Data of drained soil strength for clean sands and silts satisfy a linear relation for secant φ_{max} plotted against the logarithm of mean stress.

2. A simple modification permits plasticity calculations to deal with variable secant φ. This approach has been validated by checking the known "cohesion" solutions, N_c=5.14 for a strip footing and 5.69 for a circular punch.

3. New drained bearing capacity solutions have been derived for circular footings on dense soil, taking account of stress level effects. Comparisons with model tests on a sand and a silt show an accuracy comparable with the determination of φ in the triaxial test.

4. No actual size effects were found: stress level effects are, however, highly significant.

REFERENCES

Airey,D.W. , M.F.Randolph & A.M.Hyden (1988). The strength and stiffness of two calcareous soils. Engineering for calcareous sediments, Balkema.

Bolton,M.D. (1986).The strength and dilatancy of sands. Geotechnique 36(1):65-78.

Cox, A.D.(1962).Axially symmetric plastic deformation in soils : II . Int.J.Mech.Sci. 4:371-380.

Lau C.K. (1988). Scale effects in tests on footings. Ph.D Thesis, Cambridge University.

Shield R.T. (1955). On the plastic flow of metals under conditions of axial symmetry. Proc.Roy. Soc. of London, Series A, 233, 267-287.